https://doi.org/ 10.48047/AFJBS.6.7.2024. 665-691

African Journal of Biological Sciences

Preparation and Characterization of PVA-PAAm-PEG Blend and the Effect of CNT on the Antibacterial Activity

[1] Khansaa Saleem Sharba, [1] Golshad kheiri, [1] Mir Maqsood Golzan, [2] Khalid Haneen Abass

[1] Physics Department, Faculty of Science, Urmia University, Urmia, Iran

[2] University of Babylon, College of Education for Pure Sciences, Physics department, Iraq

Corresponding author: pure.khalid.haneen@uobabylon.edu.iq

Abstract

The PVA-PAAm-PEG polymer blend and its composite films with different weight percentages of carbon nanotubes (CNTs) were synthesized using the solution-cast technique. CNTs were added in varying amounts (0.005 g, 0.010 g, 0.015 g, and 0.020 g). Fourier-transform infrared spectroscopy (FTIR) was used to structurally investigate the fabricated nanocomposite films and detect the bonding and reaction types between the polymeric blend and CNTs. The results indicate that no chemical reactions occurred; instead, there was only physical blending, and no new interatomic bonding formed. Scanning electron microscopy (SEM) confirmed a strong dispersion of CNTs on the surface of the polymeric matrix. bsorbance spectra were determined in the wavelength range of 200-800 nm. The absorption increased with the increasing concentration of carbon nanotubes (CNTs). The optical energy gap of the fabricated films decreased with increasing CNT content, from 4.8 eV to 3.6 eV. This reduction in energy gap makes the composite desirable for use in the semiconductor industry. Additionally, the refractive index increased with the addition of CNT. Regarding the A.C. electrical properties, the dielectric constant and dielectric loss increased with higher CNT nanoparticle concentrations, while they decreased with increasing frequency of the applied electric field. On the other hand, the A.C. conductivity exhibited a significant rise as the frequency of the electric field increased for all samples. At 102 Hz, the conductivity showed a proportional increase with the rising weight percentage of CNTs. Furthermore, the antibacterial activity of this system was examined using E. coli bacteria. It was found that the inhibition zone increased with the higher CNT content in the polymeric blend.

Keywords: PVA- PAAm-PEG:CNT, casting technique, structural properties, E. coli bacteria.

Introduction

Nanocomposites are a crucial topic in polymer nanomaterials. They have been developed to exhibit distinct physicochemical properties [1]. The interfacial interactions and fine dispersion of nanofillers within the polymer matrix are considered the most important factors contributing to the enhancement of nanocomposite properties [2]. As polymer properties improve, their applications depend on the contribution of nanomaterials to the overall performance [3]. Polymeric nanocomposites have attracted considerable research interest due to their high strength-to-weight ratio, excellent corrosion resistance, affordability, and ease of fabrication into complex shapes [4]. Different nanometric fillers have been employed to enhance the mechanical performance, thermal conductivity, and electrical conductivity of polymeric matrices. Typically, these materials include fillers in the form of fibers or various types of particles [5]. Polymers can be classified into two main groups: natural and synthetic. Natural polymers include proteins, cellulose, starches, and rubber. On the other hand, synthetic polymers encompass materials like poly (vinyl chloride), nylons, polyethylene, polypropylene, and polyester polycarbonate, etc. [6].

Polyvinyl alcohol (PVA), which is derived from polyvinyl acetate through hydrolysis, is easily biodegradable by biological organisms and soluble in water [7]. This biopolymer is also a suitable material for biomedical applications, particularly in drug delivery, making it highly relevant in the field of bio applications [8]. PVA is a non-toxic, water-soluble, highly crystalline, lightweight, and biocompatible polymer. It exhibits interesting physical and chemical properties, and its abundance of hydroxyl groups (OH) allows it to be prepared as a film [9]. PVA is a polymer with a carbon chain backbone, to which hydroxyl groups are attached via methane carbons. These OH groups can serve as a source of hydrogen bonding, thereby facilitating the formation of polymer mixtures.

[10, 11]. PVA is a polymer that was investigated by a group of researchers who studied its properties well because it is used in many important applications and various fields such as electrochromic windows, sensors, bio-medical fields, fuel cells, etc. PVA has some other properties that are distinguished from other polymers such as high mechanical strength, corrosion resistance, and good thermal stability [12].

Polyacrylamide (PAAm) is a water-soluble polymer with a wide range of industrial flocculant applications. PAAm and its derivatives have gained attention in recent years due to their high molecular weight, ability to dissolve in water without forming a monomer, and their non-toxicity. Their copolymers with other hydrophilic monomers and metallic salts are used in various applications, including mining, water treatment, and other fields [13]. PAAm is often used to increase the viscosity of water, polyamides, and solid acrylic materials. The presence of aggregates of amine and carboxyl groups in the dry polymer chains leads to strong hydrogen bonding between chains, resulting in a highly stable material. Due to the bonded hydrogen molecules and differences in the hydrogen profile, bonded polyamides become more effective in increasing strength and cohesion. These properties make them suitable for forming fibers, commonly known as nylons. However, it's important to note that their mechanical characteristics include weak tensile strength, poor resistance to pressure, and limited elongation [14].

Polyethylene glycols (PEG), are liquid or solid polymers of the general formula H $OCH_2CH_2)n\cdot OH$ [15]. For improved elasticity, additional polymers can be incorporated. When a plasticizer is added, it reduces the molecular rigidity by weakening the intermolecular forces along the polymer chain [16]. For this purpose, PEG cannot be used to prepare films without a plasticizer or without adding other polymers. Poly (ethylene glycol) PEG has a flexible structure of C–O–C bonds and is an essential

type of water-soluble thermoplastic. Moreover, PEG exhibits solubility in water and organic solvents, high hydrophilicity, crystallinity, and self-lubricating properties. Therefore, PEG is one of the most preferred polymers for various significant applications, such as solid polymer electrolytes in sensors and batteries [17].

CNTs are allotropes of carbon. They consist of tubular structures made of graphite. CNTs exhibit various novel properties that render them valuable in nanotechnology and pharmaceutical applications. With diameters measured in nanometers and lengths spanning several millimeters, they possess a wide range of electronic, thermal, and structural characteristics. These properties vary based on the specific type of nanotube, which can be defined by its diameter, length, chirality, twist, and wall structure. The unique surface area, stiffness, strength, and resilience of CNTs have generated significant excitement in the field of pharmacy [18]. Nanofillers, particularly carbon nanomaterials, have significantly enhanced properties even at very low loading levels when integrated into polymer matrices. Notably, polymer composites CNTs and graphene have found diverse applications in modern science and technology. These fillers impart unique properties to the polymer matrices [19]. Graphene has garnered special attention due to its unique properties[20]. It is derived from natural graphite and is more cost-effective compared to other fillers, such as CNT [21]. The new research deals with the synthesis of innovative nanocomposites (PVA-PAAm-PEG:CNT) by studying their structural and optical properties, for antibacterial activity.

Experimental Part

Materials

The polymers; PVA (Mol wt = 18,000 g/mol), with high purity (99.0%) (Panreac\Spain, Lnc) Barcelona Espana, PAAm (Mol wt = 5×10^6

g/mol) with high purity (99.99 %) by a company (British Drug Houses (BDH)) and PEG from (Reagent World) with (6000 Dalton Mw and purity 99.8%) are used in the form of granules. The additive nanomaterials were CNT (Purity 90%, Diameter 100 nm, Length 10 μm) with varying percentages.

preparation of PVA- PAAm-PEG: CNT nanocomposites

Polymer nanocomposite films were prepared by mixing 40% PAAm in 60 mL of distilled water in a glass beaker equipped with a magnetic stirrer. The mixing process continued for 45 minutes to obtain a more homogeneous solution at a temperature of 90 ºC. The 40% PVA was added to the mixture and waited for 1 h for a homogenous solution mixture with a temperature of 90 ºC. Next, 20% PEG was added to the mixture, and it was allowed to homogenize for 1 hour at a temperature of 90 ºC. The temperature of the PVA-PAAm -PEG matrix was reduced to about 25 ºC before adding four ratios (0, 0. 5, 1.0, 1.5, and 2.0) wt.% of CNT for 1 h of each case to prepare PAAm-PVA-PEG:CNT nanocomposite films, as shown in Table (1). They cast each of these ratios into a petri dish (5 cm in diameter) to create the films. The entire set is placed in a dust-free room, and the solvent is allowed to evaporate into the air at room temperature over the course of 7 days. Afterward, the film is carefully peeled from the petri dish.

Table 1: Summarized the preparation of PVA-PAAm-PEG and PAAm-PVA-PEG:CNT Nanocomposites.

Smples No.	PVA (g)	PAAm (g)	PEG (g)	CNT (%)
1	0.4	0.4	0.2	0.0
2	0.398	0.398	0.199	0.5
3	0.396	0.396	0.198	1.0

4	0.394	0.394	0.197	1.5
5	0.392	0.392	0.196	2.0

Results and Discussion

The Fourier transform infrared (FTIR) test was used to determine changes in the bonds and the formation of new bonds in the PVA-PAAm-PEG blend. Figure 1 represents the FTIR of PVA-PAAm-PEG: CNT nanocomposites with varying ratios of CNT. These spectra were recorded at room temperature in the wavenumber optical range of 4000-500 cm^{-1} . The spectra exhibited characteristic bands of stretching and bending vibrations of the functional groups formed in the composites. From these spectra, it can be noted that the absorption peaks at approximately 3290.92 and 3292.57 cm^{-1} were attributed to the stretching vibration of a hydroxyl group (OH) in the polymer matrix chain [22]. The absorption peaks at 2895.29, 2893.09, 2890.43, 2891.25, and 2891.20 cm^{-1} were attributed to methylene (C-H) stretching, while the bands at 1732.71 and 1733.16 cm^{-1} were attributed to carboxylic acid (C=O) stretching. [23]. Meanwhile, the functional groups at 1240.67, 1240.68, 1240.61, 1240.40, and 1239.69 cm^{-1} are all attributed to carbon dioxide (C-O) stretching [24]. At 1090.50, 1099.82, 1107.07, and 1101.25 cm^{-1}, the peaks are recognized as (C-C) stretching vibrations [25]. The FTIR spectra exhibit a shift in peak position, as well as changes in shape and intensity compared to pure PVA-PAAm-

PEG films. Notably, the peak at 3300 cm^{-1}, which corresponds to the PVA polymer and represents the (OH) stretching vibration bond, does not appear in these spectra. Instead, the peaks at 3290.92, 3292.57, and 3292.87 cm^{-1}, attributed to (OH) stretching vibrations, are observed. Additionally, the peak at 1141 cm^{-1}, which corresponds to the PVA polymer, represents the C-O stretching bond. However, the peak at 1323 cm^{-1}, associated with the PAAm polymer, did not appear in these spectra. Instead, peaks at 1240.67, 1240.68, 1240.61, 1240.40, and 1239.69 cm^{-1} were observed, indicating (C-O) stretching [26, 27]. There is a noticeable shift in the (C-H) stretching bond, which represents both PVA and PAAm polymers. These peaks occur at 2895.29, 2893.09, 2890.43, 2891.25, and 2891.20 cm^{-1}, instead of the usual 2940 cm^{-1} and 2931 cm^{-1} bonds associated with the same polymer, which also correspond to (C-H) stretching. Furthermore, there is a noticeable shift in the (C=O) stretching bond, which represents the PVA polymer. This shift results in peaks at 1732.71 and 1733.16 cm^{-1}, instead of the usual 1731 cm^{-1} bond associated with the same polymer, which also corresponds to (C=O) stretching. Additionally, there is a similar shift in the (C-C) stretching bond for the PVA polymer. These new peaks occur at 1090.50, 1099.82, 1107.07, and 1101.25 cm^{-1}, rather than the standard 1087 cm^{-1} bond, which also corresponds to (C-C) stretching [27,28]. It is evident that there is a decrease in transmittance as the proportion of CNT increases. The higher film density results in an increased presence of atoms and ions along the light path, leading to enhanced absorbance in the UV and IR regions. This phenomenon is illustrated in figures (2) and the corresponding images (B, C, D, and E). Based on the FTIR analysis, it appears that there is no chemical reaction between the carbon nanotubes (CNT) and the polymeric blend. Instead, the interaction seems to be purely physical blending. This conclusion is drawn from the absence of specific bonds associated with the nanocomposite, as well as the lack of any

additional peaks in the IR spectra. These findings align with the observations made by previous researchers [29].

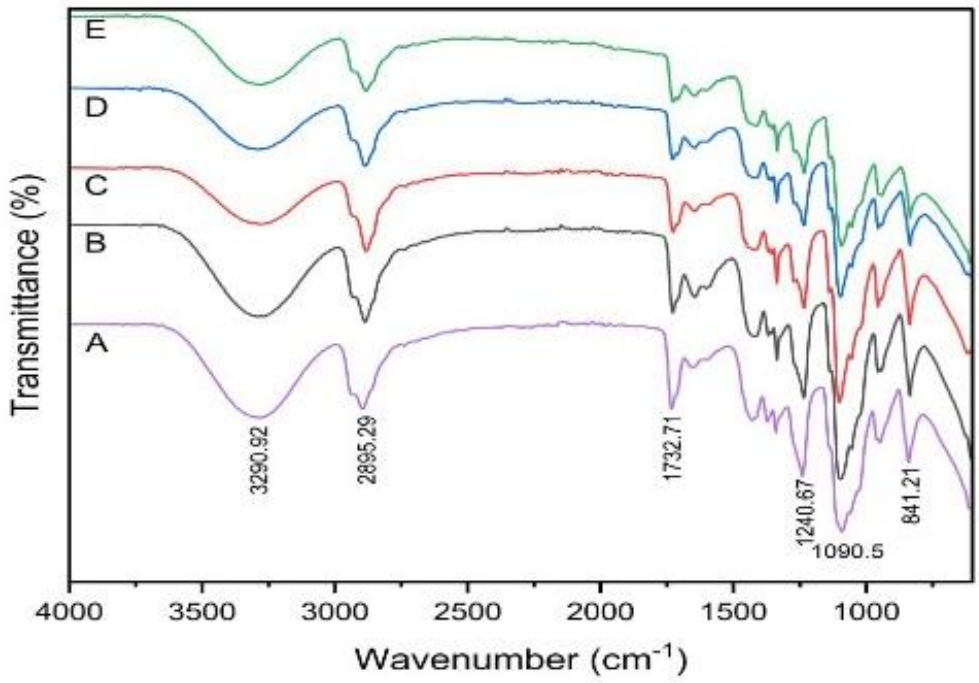

Figure1. FTIR spectra of PVA-PAAm-PEG:CNT with various content of CNT: (A) 0 wt.% (B) 0. 5 wt.% (C) 1 wt.% (D) 1.5 wt.% and (E) 2 wt.%.

Figure 2 shows a scanning electron microscopy (SEM) micrograph of the surface of the PVA-PAAm-PEG blend and the PAAm-PVA-PEG: CNT nanocomposite films at a magnification of 7000X. From images A and B in Figure 2, a uniform morphology reveals a rather soft surface. In Figure 2 (C, D, and E), the increase in the ratio of CNT in a polymer matrix for the PAAm-PVA-PEG:CNT nanocomposites led to changes in the surface morphology and increased roughness. The nanocomposite films show some CNTs that were finely dispersed without aggregates, with a well-distributed presence on the surface. This may indicate the occurrence of a homogeneous growth mechanism. In SEM images, the size of the CNTs was measured on the surface of the nanocomposites. The particle sizes of

the CNTs ranged from 339.7 nm in dimensions. These results agree with the optical microscopy images.

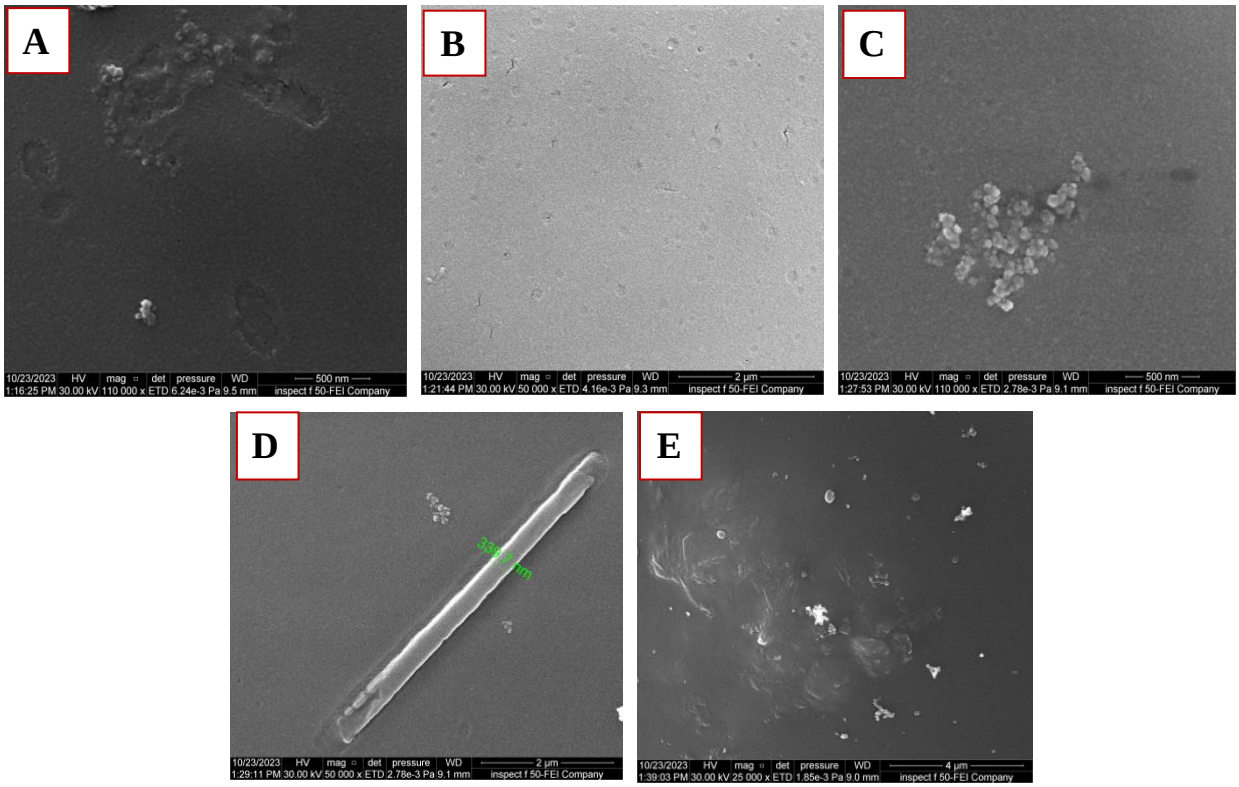

Figure (2): SEM images of PVA-PAAm-PEG:CNT with various content of CNT and magnifications (A) 0 wt.% (B) 0. 5 wt.% (C) 1 wt.% (D) 1.5 wt.% and (E) 2 wt.%.

Figure 3 shows the UV-Visible absorption spectra of PVA-PAAm-PEG:CNT nanocomposites with varying CNT content in the wavelength range of 200-800 nm, recorded at room temperature. According to the spectra, it is noticeable that all of the films exhibit high absorbance in the UV region and low absorbance in the visible region. This behavior can be explained as follows: at longer wavelengths, the incident photons do not have enough energy to interact with atoms, resulting in photon transmission. When the wavelength decreases (at the neighborhood of the fundamental absorption edge), the interaction between an incident photon and the material will occur, and the photon will be absorbance. The

absorbance increases with the increasing weight percentages of the nanomaterials. This is due to absorb the incident light by free electrons. The results agree with the results of the previous researchers [30].

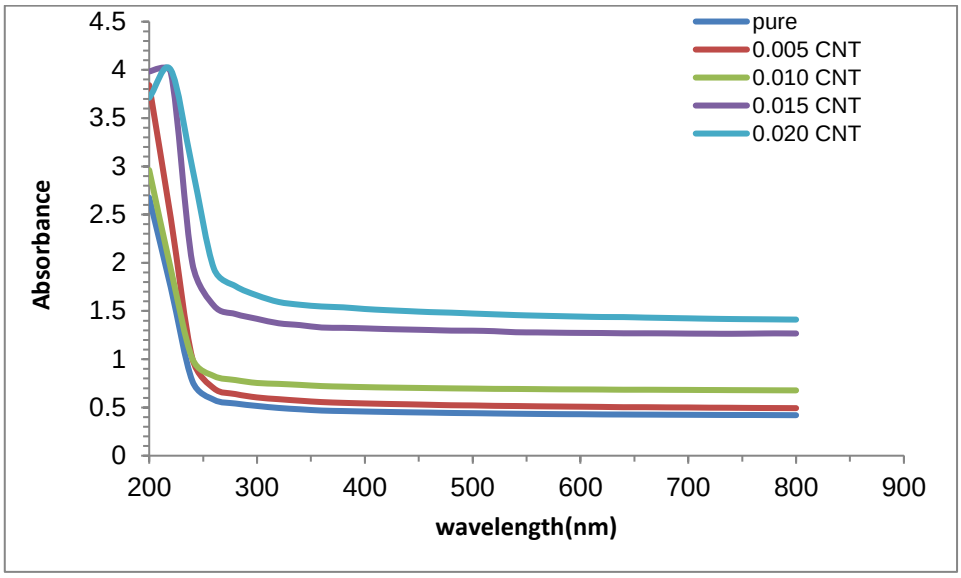

Figure 3. The absorbance spectra as a function of wavelength of PVA-PAAm-PEG blend and PVA-PAAm-PEG:CNT nanocomposites.

The absorption coefficient of the blended polymers and its nanocomposite films was calculated from the region of high absorption at the fundamental absorption edge using Lambert Beer's law [31]:

$$\alpha = 2.303 \frac{A}{t} \qquad (1)$$

A and t refer to the absorbance and thickness of the samples, respectively. Figure 4 shows the absorption coefficient (α) as a function of photon energy for the PVA-PAAm-PEG blend with varying CNT concentrations. It is evident that the absorption coefficient is smallest at low energy. This indicates that the likelihood of electron transition is low because the energy of the incident photon is insufficient to move the electron from the valence band to the conduction band. Conversely, at higher energies, absorption is greater, signifying a higher probability of

electron transitions. Consequently, the energy of an incident photon is adequate to move the electron from the valence band to the conduction band. The energy of the incident photon exceeds the forbidden energy gap, indicating that the absorption coefficient provides insights into the nature of electron transitions. When the absorption coefficient values are high at higher energies, it suggests a greater likelihood of electron transitions (α >104 cm-1). It is expected that direct transitions of electrons occur, with energy and momentum being maintained by the electrons and photons. However, when the absorption coefficient values are low ($\alpha < 10^4$ cm^{-1}) at low energies, indirect electron transitions are expected. In this case, electronic momentum is maintained with the assistance of phonons. These results align with the findings of previous researchers. [32].

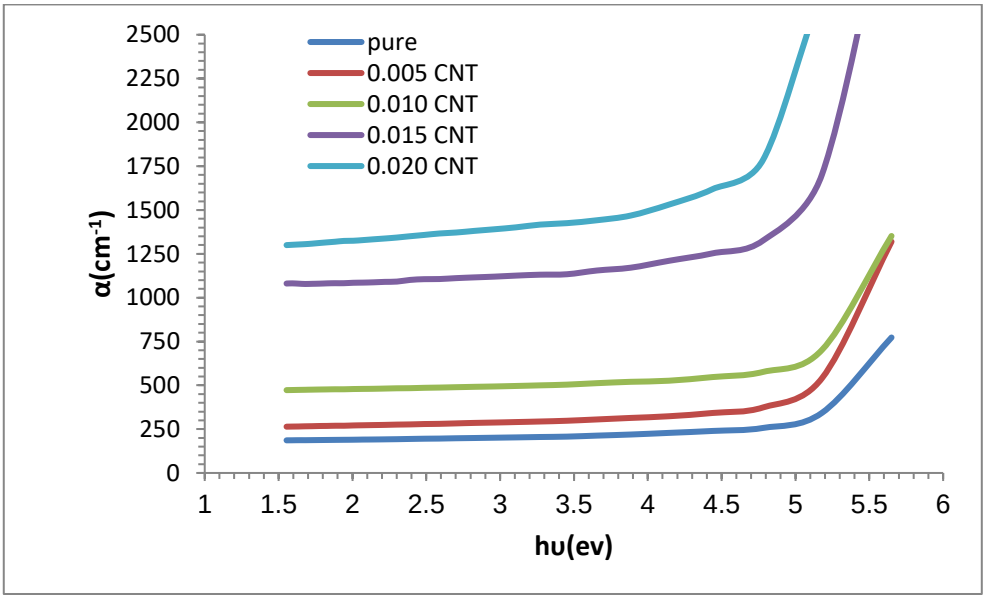

Figure 4. The absorption coefficient relation with the energy of PVA- PAAm-PEG blend and PVA- PAAm-PEG :CNT nanocomposites.

Energy band gaps of the films were calculated using the Tauc relation (2) [33,34]

$$\alpha h\upsilon = B(h\upsilon - Eg^{opt} \pm E_{ph})^{r} \qquad (2)$$

E^{ph} represents the phonon energy, with a negative sign (-) applied for phonon absorption and a positive sign (+) used for phonon emission. The exponential constant is denoted as 'r' in the equation, where its value is determined by the transitions: r = 2 for allowed indirect transitions and r =3 for forbidden indirect transitions. When r = 2, the allowed indirect transition band gap is calculated, whereas r = 3 corresponds to the forbidden indirect transition band gap. [27].

Figure 5 shows the relation between absorption edge $(\alpha hv)^{1/2}$ of PVA-PAAm-PEG:CNT nanocomposites as a function of photon energy, with drawing a straight line (extrapolation) from the upper part of the curve toward the x-axis at the value $(\alpha hv)^{1/2} = 0$, it gets the energy gap for the allowed indirect transition [35]. The obtained values are shown in Tables (2). The energy gap values decrease with increasing weight percentages of CNT. This phenomenon is attributed to the creation of site levels within the forbidden energy gap. The transition occurs in two stages: electrons transition from the valence band to local levels and then to the conduction band as the CNT weight percentage increases. This behavior is attributed to the heterogeneous nature of nanocomposites, where electronic conduction depends on the added materials. The increased presence of CNTs provides electronic pathways within the polymer, facilitating the movement of electrons from the valence band to the conduction band. This phenomenon explains the decrease in the energy gap with increasing CNT content. The results align with those of previous researchers [36].

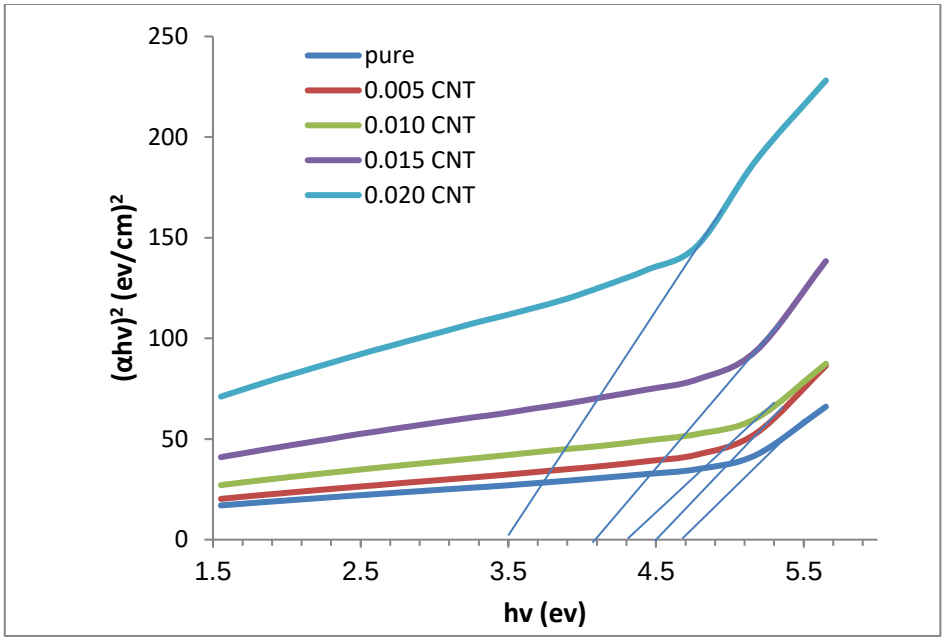

Figure5. Optical energy gap of the allowed indirect transition with the energy of PVA- PAAm-PEG:CNT nanocomposites.

Table 2. The values of energy gap of the allowed indirect transition of PVA-PAAm-PEG:CNT nanocomposites.

Samples	Allowed indirect transition (eV)
PVA-PAAm-PEG	4.7
PVA-PAAm-PEG 0.5% CNT	4.5
PVA-PAAm-PEG 1% CNT	4.3
PVA-PAAm-PEG 1.5% CNT	4.1
PVA-PAAm-PEG 2% CNT	3.5

The refractive index (n) is calculated using equation 3 [37,38]:

$$n = \sqrt{\frac{4R - k^2}{(R-1)^2}} - \frac{(R+1)}{(R-1)} \qquad (3)$$

Figure 6 illustrates the change in the refractive index of PVA-PAAm-PEG:CNT nanocomposites as a function of wavelength. The data reveals that the refractive index increases with higher weight percentages of CNT

concentration in the polymers. This behavior is attributed to the increased density of nanocomposites. When incident light interacts with a sample that exhibits high refractivity in the UV region, the refractive index values increase. These results align with those of previous researchers [39,40].

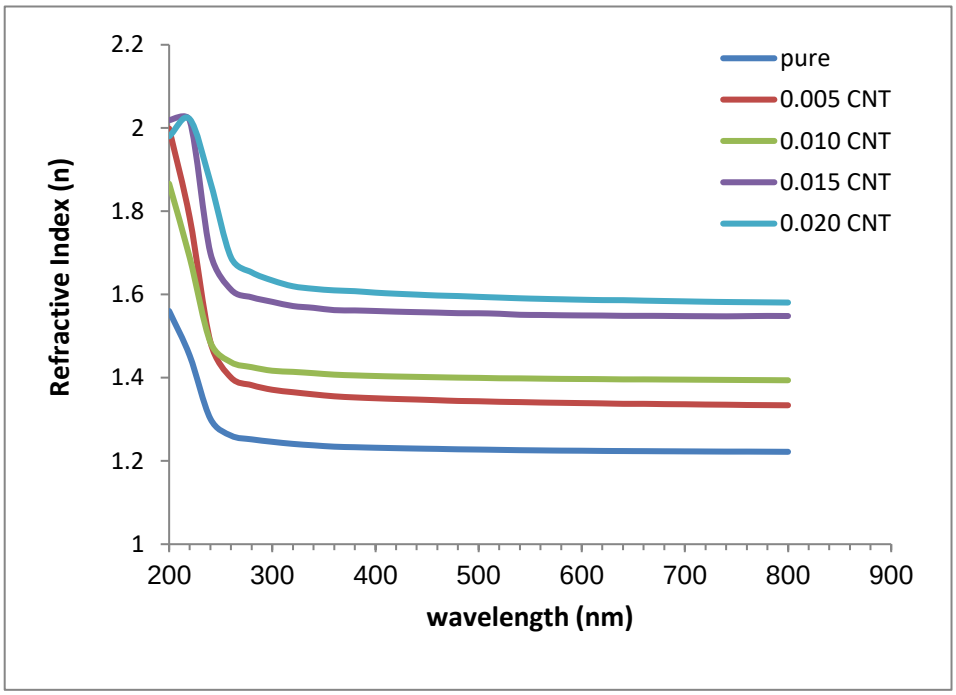

Figure 6. The refractive index (n) as a function of wavelength of PVA- PAAm-PEG blend and PVA- PAAm-PEG:CNT nanocomposites.

The dielectric constant is calculated using following equation [41]:

$$\acute{\varepsilon} = Cp\ d / \varepsilon_o\ A \qquad (4)$$

which, Cp is capacitance of matter, thickness (d in cm), A= (in cm^2).

The dielectric constant of polymer blends (PVA-PAAM-PEG) and their nanocomposite films with varying concentrations (0.5, 1, 1.5, and 2) wt. % of carbon nanotubes (CNT) is illustrated in Figure (7), as a function of electric field frequency. From this figure, it is observed that higher frequencies lead to a reduction in the space charge polarization compared to the total polarization. Consequently, the dielectric constant values for all (PVA-PAAM-PEG:CNT) nanocomposite samples decrease. This indicates

that at lower frequencies, the space charge polarization plays a more significant role in the overall polarization. The maximum dielectric constant, are (0.4, 0.46, 0.53, 0.61and 0.7) for polymer blend and its NCs with different (0.005, 0.010 , 0.015 and 0.020) wt.% of CNT at 100Hz, respectively. The magnitude of dielectric constant indicates the ability of the material to store energy from the applied electric field.

Figure 8 depicts the relationship between the dielectric constant and the concentration of carbon nanotubes (CNT) at a frequency of 100 Hz. The figure demonstrates that the dielectric constant of nanocomposites rises in proportion to the concentration of CNTs. The observed phenomenon can be attributed to the interfacial polarization occurring within the nanocomposites when subjected to an alternating electric field, as well as the augmentation of charge carriers [42].

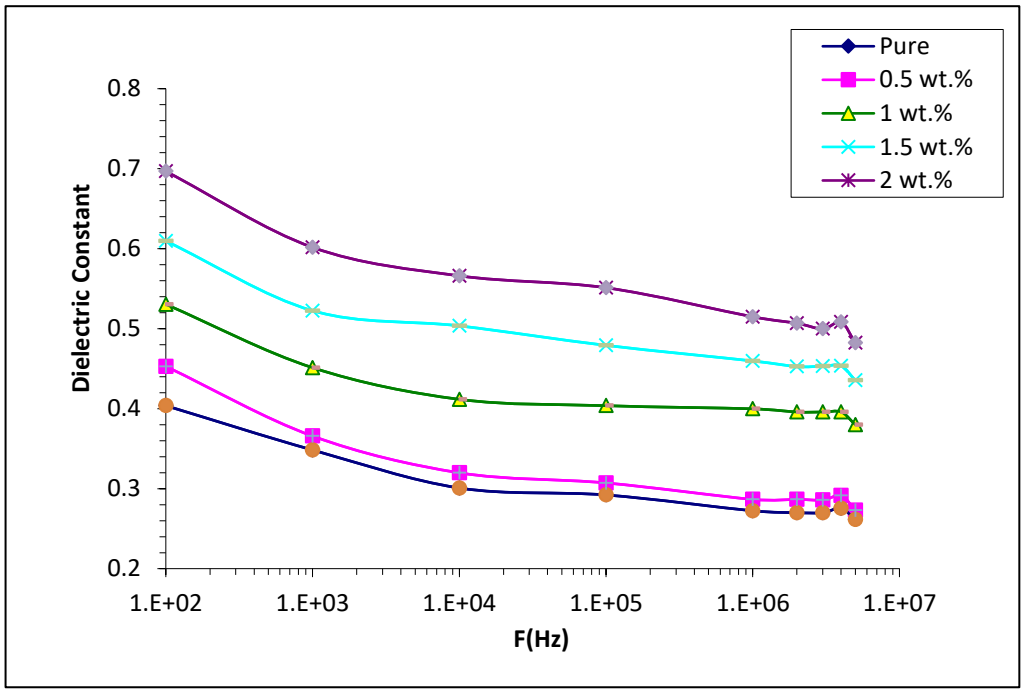

Figure 7. Variation of dielectric constant Wavelength of PVA-PAAm-PEG Blend and PVA- PAAm-PEG:CNT nanocomposite with frequency at RT.

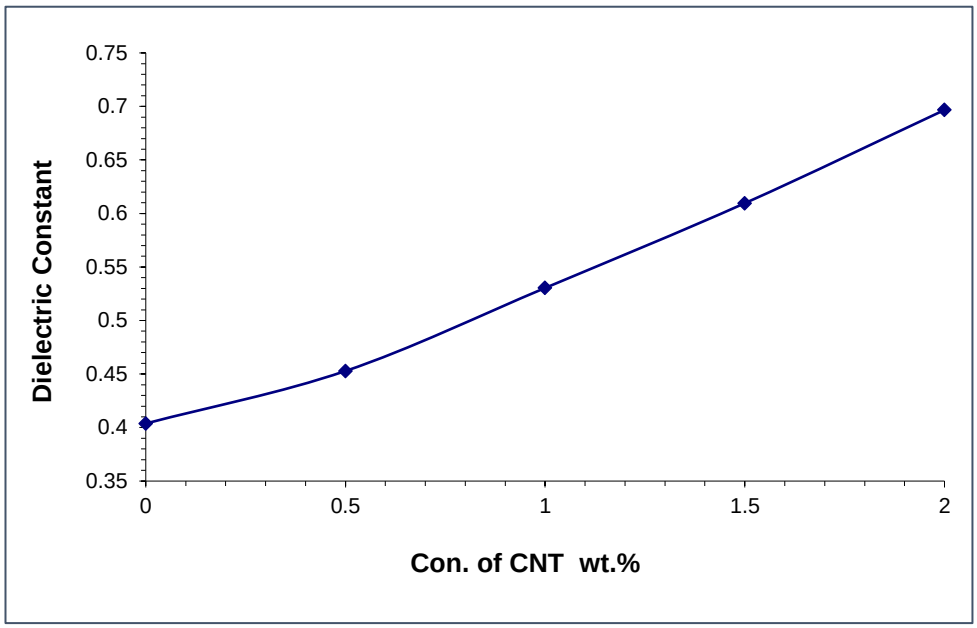

Figure 8. Effect of CNT concentrations on dielectric constant of PVA-PAAm-PEG Blends at 100Hz.

The dielectric loss measures the lost electrical energy in the sample from the applied field which is transformed to thermal energy in the sample. The dielectric loss of nanocomposites is calculated by using following equation [43]:

$$\varepsilon'' = \acute{\varepsilon}\, D \qquad (5)$$

The relationship between the dielectric loss and the electric field frequency of carbon nanotubes (CNTs) in the (PVA-PAAM-PEG) blends at room temperature (RT) is illustrated in Figure 9. The data indicates that the dielectric loss of the nanocomposites decreases as the frequency of the electric field increases across all samples. This behavior is attributed to a reduction in the contribution of space charge polarization. Furthermore, the nanocomposite films containing 2 wt.% CNTs exhibit a maximum dielectric loss of 0.49 at a low frequency of 10^2 Hz

Figure 10 demonstrates that the dielectric loss of nanocomposites composed of carbon nanotubes (CNTs) increases as the concentration of

nanoparticles rises. This behavior is attributed to the augmentation of the quantity of charge carriers. Analogous conduct was documented in [44,45].

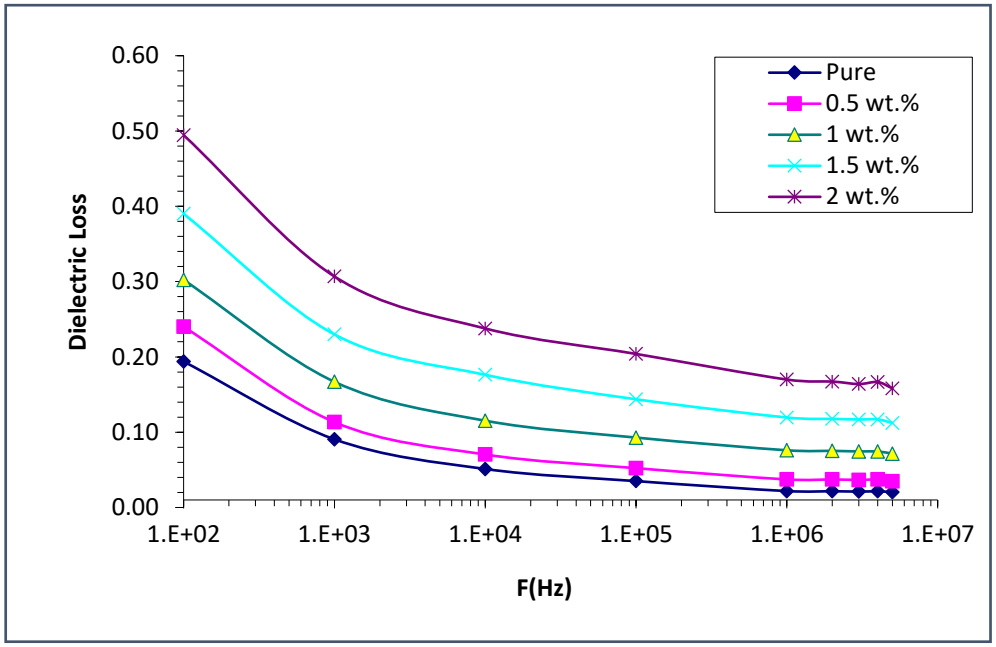

Figure 9.Variation of dielectric loss of PVA-PAAm-PEG Blend and PVA-PAAm-PEG:CNT nanocomposite with frequency at RT.

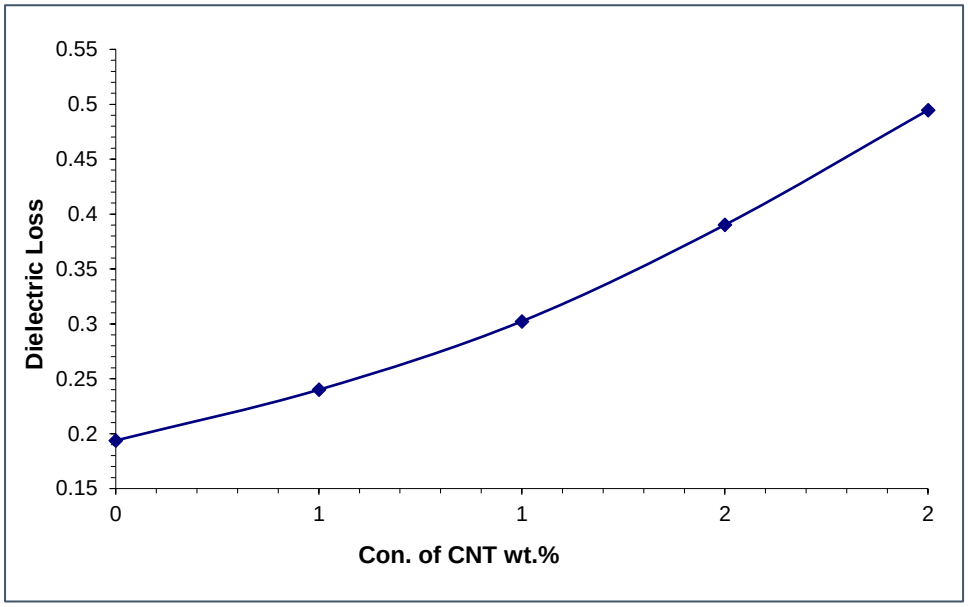

Figure 10. Effect of CNT concentrations on dielectric loss of (PVA-PAAM-PEG) Blends at 100Hz.

The A.C electrical conductivity ($\sigma_{A.C}$) of nanocomposites is calculated by using following equation [46]:

$$\sigma_{A.C} = 2\pi f \acute{\varepsilon} D \varepsilon_o \qquad (6)$$

The relationship between the A.C electrical conductivity and the frequency of the electric field is demonstrated in Figure (11) for carbon nanotubes (CNT) in the PVA-PAAM-PEG blends at room temperature (RT). The A.C conductivity exhibits a significant rise as the frequency of the electric field increases for all samples. This phenomenon can be attributed to the polarization of space charge at low frequencies and the movement of charge carriers through a hopping process[45].

Furthermore, the conductivity of the PVA-PAAM-PEG blends at 10^2 Hz is shown to rise proportionally with the increasing weight percentage of CNT, as depicted in Figure (12). The addition of nanoparticles to the composition of the nanocomposite increases its conductivity by increasing the number of charge carriers. This, in turn, reduces the resistance of the nanocomposite and leads to an increase in its AC electrical conductivity. Analogous conduct was documented in [45].

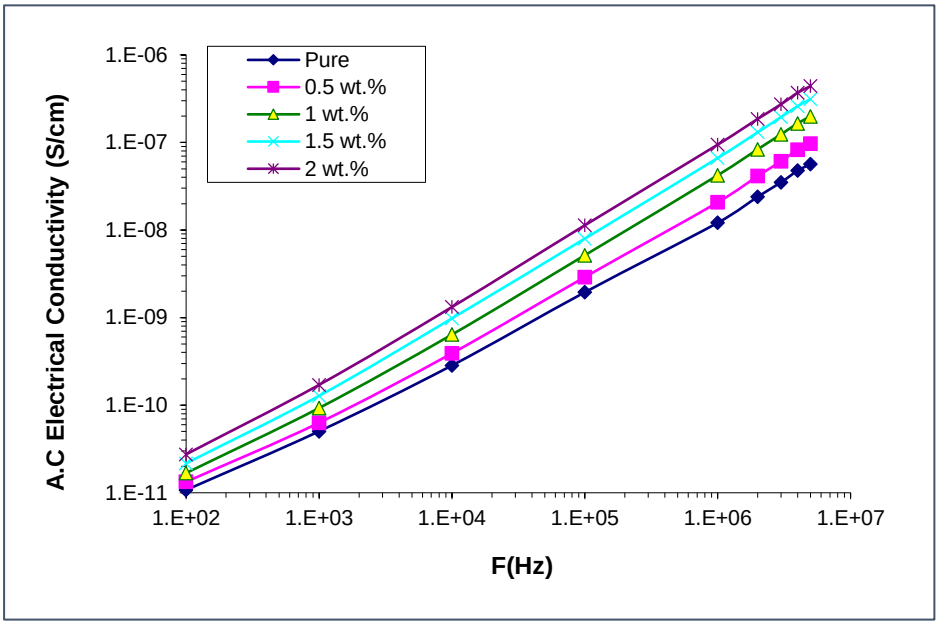

Figure 11. Variation of A.C electrical conductivity of PVA-PAAm-PEG Blend and PVA- PAAm-PEG:CNT nanocomposite with frequency at RT.

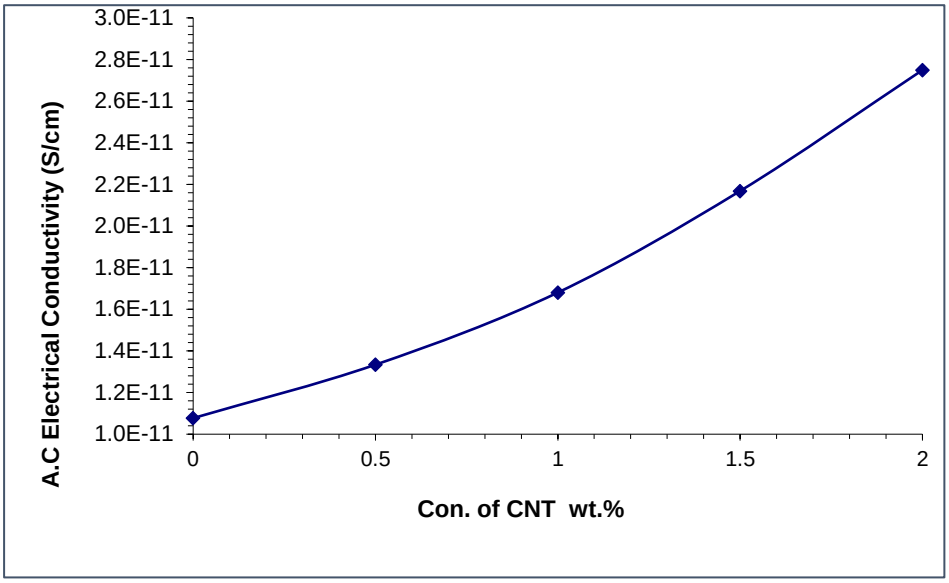

Figure12. Effect of CNT nanoparticles concentrations on A.C electrical conductivity of (PVA-PAAM-PEG) blend at 100Hz.

4.1Anti-bacterial activity Application

Nanoparticles are considered a promising substitute for antibiotics because of their capacity to exhibit a broad-spectrum antibacterial effect even at minimal concentrations. This research evaluated the efficacy of nanocomposites comprising PVA-PAAm-PEG and CNT with varying levels of CNT (0, 0.5, 1.5, and 2) against Escherichia coli, a Gram-negative bacterial strain. the antibacterial susceptibility was assessed by measuring the diameter of inhibition zones. As illustrated in Figure 7, there was a distinct variance in the bacterial inhibition zones among E. coli colonies when comparing the pure polymer blend to its nanocomposites. While no bacterial inhibition zone was observed in the pure polymeric mixture, the addition of nanoparticles to the polymer blend enhanced the bacterial resistance sensitivity. The order of inhibition zones for the samples was as follows:

PVA-PAAm-PEG < PVA-PAAm-PEG:0.5% CNT < PVA-PAAm-PEG:1.0% CNT < PVA –PEG:1.5% CNT < PVA-PEG:2.0% CNT. The results indicate that the diameter of the inhibition zone reaches its peak value of 18 mm when the CNT content in the polymer matrix is at its highest level (0.02 g). Conversely, the diameter of the inhibition zone drops to about 12 mm when the CNT content is at its lowest level of 0.005 g. For a CNT content of 0.010 g, the diameter of the inhibition zone measures approximately 14 mm, and at 0.015 g, it expands to around 17 mm. This study suggests that nanocomposite films effectively hinder the growth of E. coli. The main mechanism behind the antibacterial properties of these nanocomposites is likely the production of reactive oxygen species, specifically oxidative stress triggered by reactive oxygen radicals (ROS). ROS comprises radicals like hydrogen superoxide, hydroxyl radicals (-OH), and (O^{-2}) radicals (H_2O_2), which inflict harm on the DNA and proteins of bacteria[47]. These findings are noteworthy for applications in biosensors and bacterial disinfection.

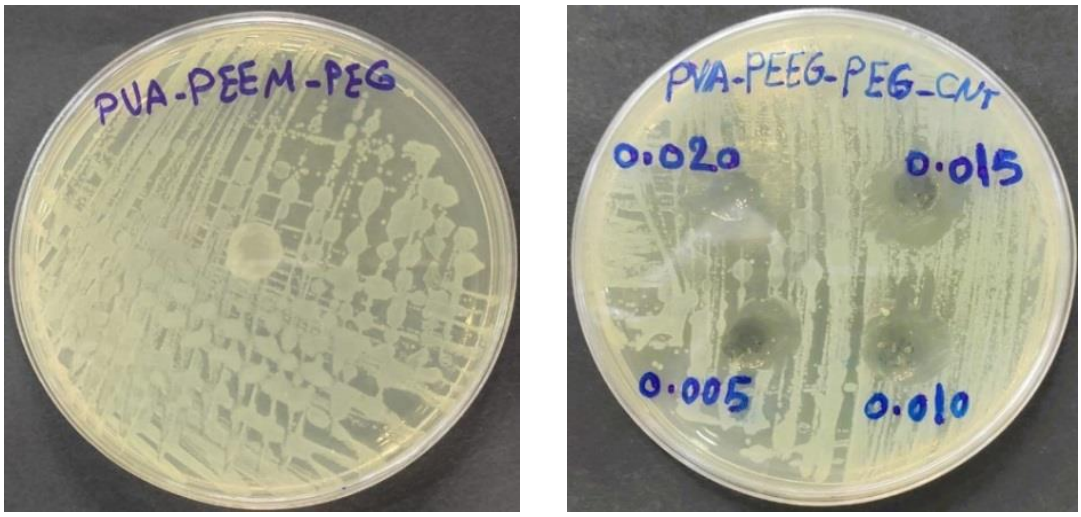

Figure 13. Images for inhibition zones of PVA- PAAm-PEG blend and PVA-PAAm-PEG:CNT nanocomposites on E. coli.

Conclusions

The PVA-PAAm-PEG:CNT mixture was successfully prepared using the casting method. Optical microscopy images exhibited a uniform and

thorough dispersion of the nanomaterial within the films. The FTIR spectra displayed shifts in certain bands and alterations in the intensities of other bands when compared to the PVA-PAAm blend film. Scanning electron microscopy (SEM) was employed to analyze the compatibility among the different components of the polymers and nanomaterials, providing insight into the surface morphology of the PVA-PAAm-PEG:CNT nanocomposite films. An increase in the proportion of CNT is correlated with a decrease in permeability. The absorbance, absorption coefficient, and refractive index of PVA-PAAm:CNT nanocomposites elevate as the concentrations of CNT increase. Furthermore, the optical energy gap of the fabricated nanocomposites experiences a decrease with the rising presence of CNT nanoparticles, reducing from 4.7 to 3.5 eV.

The dielectric constant and dielectric loss of PVA-PAAM-PEG:CNT nanocomposites increase with higher concentrations of CNT nanoparticles and decrease with an increase in the frequency of the applied electric field. Conversely, the A.C conductivity demonstrates a notable increase as the electric field frequency rises in all samples, with a proportional increase in A.C conductivity at 102 Hz observed with higher weight percentages of CNT due to an increased number of charge carriers. Moreover, increasing the NP content in the PVA-PAAm-PEG:CNT mixture results in an expansion of the inhibition zone diameter against Escherichia coli, enhancing its antibacterial application.

References

[1] Dhillon A and Kumar D (2018). Recent advances and perspectives in polymer-based nanomaterials for Cr (VI) removal. In: New polymer nanocomposites for environmental remediation. Amsterdam, Netherlands: Elsevier,29–46.

[2] Molaei P and Kazeminezhad I (2019). One-step in situ synthesis of antimony sulfide/reduced graphene oxide composite as an absorber layer with enhanced photocurrent performances for solar cells. J Nanopart Res; 21: 1–12.

[3] Firdaus RM, Rosli NIM, Ghanbaja J, et al (2019). Enhanced adsorption of methylene blue on chemically modified graphene nanoplatelets thanks to favorable interactions. J Nanopart Res; 21: 1–8.

[4] B. Debelak, K. Lafdi (2007), use of exfoliated graphite filler to enhance polymer physical properties, Carbon N. Y. 45 (9).1727–1734,

[5] Khammassi S, Tarfaoui M. (2020), Influence of exfoliated graphite filler size on the electrical, thermal, and mechanical polymer properties, J. Compos. Mater. 54 (25). 3731–3741.

[6] Mark JE. Polymer Data Handbook (2001). 2nd ed. New York, USA: Oxford University Press, Inc; 1999.

[7] Razzak, M.T.; Darwis, D.; Zainuddin; Sukirno. Irradiation of polyvinyl alcohol and polyvinyl pyrrolidone blended hydrogel for wound dressing. Radiat. Phys. Chem, 62, 107–113.

[8] Dash, M.; Chiellini, F.; Ottenbrite, R.M.; Chiellini, E. Chitosan (2011). A versatile semi-synthetic polymer in biomedical applications. Prog. Polym. Sci, 36, 981–1014.

[9] Zbala, A.A.K., Al-Ogaili, A.O.M., Abass, K.H., "Effect of Adding Silver Nanoparticles on Structural and Microscopic Properties of PAAm-PEG Polymer Blend", Journal of Nanostructures, 2022, 12(4), pp. 892–897.

[10] Rajendran S., Sivakumar M., and Subadevi R. (2004), “Investigations on the effect of various plasticizers in PVA–PMMA solid polymer blend electrolytes,” Mater. Lett.,58,5,641–649.

[11] J. H. Lee, H. B. Lee, and J. D. Andrade (1995), “Blood compatibility of polyethylene oxide surfaces,” Prog. Polym. Sci., 20, 6,1043–1079.

[12] Rajendran S., Sivakumar M., and . Subadevi R (2004), “Investigations on the effect of various plasticizers in PVA–PMMA solid polymer blend electrolytes,” Mater. Lett.,8, 5,641–649.

[13] Herth G., Schornick G., and Buchholz F. L. (2015), “Polyacrylamides and Poly (Acrylic Acids),” Ullmann’s Encycl. Ind. Chem.,1–16, doi: 10.1002 /14356007.a21_143.pub2.

[14] Zbala, A.A.K., Mousa Al-Ogaili, A.O., Abass, K.H. (2022), "Optical Properties and Dispersion Parameters of PAAm-PEG Polymer Blend Doped with Antimony (III) Oxide Nanoparticles", NeuroQuantology, 20(2), 62–68.

[15] Buong Woei Chieng, Nor Azowa Ibrahim, Wan Md Zin Wan Yunus and Mohd Zobir Hussein (2014), "Poly (lactic acid)/Poly (ethylene glycol) Polymer Nanocomposites: Effects of Graphene Nanoplatelets", Polymers, 6, 93-104.

[16] Nadarajah, K., (2005), Dissertation, Louisiana State University Agricultural and Mechanical College, 18–22.

[17] Khalid Haneen Abass, Ashraq Mohammed Kadim, Sara Kareem Mohammed, Mohd Arif Agam (2021), "Drug Delivery Systems Based on Polymeric Blend: A Review", Nano Biomed. Eng.,13(4), 414-424.

[18] Klein R. (2012), “Laser Welding of Plastics”, John Wiley and Sons.

[19] Amin S., and Amin M.,(2011) “Thermoplastic Elastomeric (Tpe) Materials and Their Use in Outdoor Electrical Insulation”, Rev. Adv. Mater. Sci. 29,15-30.

[20] Cowie J. M. G. (1991), “Polymers: Chemistry and Physics of Modern Materials”, Glasgow.

[21] Scobbo J. J., and Goettler L. A. (2003), “Applications of polymer alloys and blends”, Kluwer Academic Publishers.

[22] Yu-Mei Yue, Kun Xu, Xiao-Guang Liu, Qiang Chen, Xiang Sheng and Pi-Xin Wang,(2008)“Preparation and characterization of interpenetration polymer network films based on poly (vinyl alcohol) and poly (acrylic acid) for drug delivery”, Journal of applied polymer science, 108(6), pp.3836-3842,

[23] Manjunath A., Deepa T., N. K (2015). Supreetha and M. Irfan, “Studies on AC Electrical Conductivity and Dielectric Properties of PVA/NH_4NO_3 Solid Polymer Electrolyte Films”, Advances in Materials Physics and Chemistry,5,295-301.

[24] Rasheed, M.H., Hashim, F.S., Abass, K.H., "Impact of Ag Nanoparticles on the Spectral and Optical Properties of Electrospun Nanofibrous Poly(vinyl alcohol)-Poly(acrylamide)", International Journal of Nanoscience, Vol.22, No.3, 2023. https://doi.org/10.1142/S0219581X23500254.

[25] Deshmukh K., Ahmad J., Hägg MB. (2014). “Fabrication and characterization of polymer blends consisting of cationic polyallylamine and anionic polyvinyl alcohol”, Ionics. 20(7), 957–67.

[26] Dweik H., Sultan W., Sowwan M., & S. Makharza (2008), “Analysis characterization and some properties of polyacrylamide copper complexes”, International Journal of Polymeric Materials, 57(3),228-244.

[27] J.C. Yu, F.G. Zhao, W. Shao, C.W. Ge, and W.S. Li (2015), “Shape-controllable and versatile synthesis of copper nanocrystals with amino acids as capping agents”, Nanoscale, 7(19),8811-8818, (2015).

[28] Mansur H.S., Sadahira C.M., A. N Souza, and A. A. Mansur, (2008). "FTIR spectroscopy characterization of poly (vinyl alcohol) hydrogel with different hydrolysis degree and chemically crosslinked with glutaraldehyde", Materials Science and Engineering: C, 28(4), 539-548.

[29] Y. L. Luo, L. L. Chen, F. Xu, and Q. S. Feng (2012), "Fabrication and characterization of copper nanoparticles in PVA/PAAm IPNs and swelling of the resulting nanocomposites", Metals and Materials International, 18(5),899-908.

[30] Chiad, S.S., Alkelaby, A.S., Sharba, K.S (2020), "Optical Conduct of Nanostructure Co_3O_4 rich Highly Doping Co3O4: Zn alloys", Journal of Global Pharma Technology, 11(7), 662-665.

[31] Alkelaby, A.S., Abass, K.H., Mubarak, T.H., Habubi, N.F., Chiad, S.S., Al-Baidhany, I (2019), "Effect of $MnCl_2$ additive on optical and dispersion parameters of poly methyl methacrylate films", Journal of Global Pharma Technology 11(4),347-352.

[32] AL-Dahash G. A., Najeeb H. N., Baqer A., and Tiama R. (2012), "The Effect of Bismuth Oxide Bi_2O_3 on Some Optical Properties of Poly vinyl Alcohol", British Journal of Science,4,117-124.

[33] Hao Y, Shih H, Munoz Z, Kemp A, Lin CC (2014) Visible light cured thiol-vinyl hydrogels with tunable degradation for 3D cell culture. Acta Biomater 10: 104- 114.

[34] Ahmed N. Al-Jamal, Karar Abdali O., Khalid Haneen Abbass, Bahaa H. Rabee,and Ehssan Al-Bermany (2023)," Silver NPs Reinforced the Structural and Mechanical Properties of PVA-PAAm-PEG Nanocomposites". AIP Conference Proceedings.

[35] Al-Jamal, A.N., Hadi, Q.M., Hamood, F.J., Abass, K.H., "Particle size effect of Sn on structure and optical properties of PVA-PEG blend", Proceedings - International Conference on Developments in eSystems Engineering, DeSE, pp. 736-740, 2019. doi: 10.1109/DeSE.2019.00137

[36] Asadi S. M. A., Hamood F. J., Abass K. H, Mohammed S. K., Hassan I. M., and Latif D. (2019), "The Effect of MgO Nanoparticles on Structure and optical Properties of PVA-PAAm Blend", Research Journal of Pharmacy and Technology, 12(6),2768-2771.

[37] Abass H.K., Haidar O.N. (2019), "0.006wt.%Ag-Doped Sb_2O_3 Nanofilms with Various Thickness: Morphological and optical properties", Journal of Physics: Conference Series, 1294(2).

[38] Sharba, K.S., Alkelaby, A.S., Sakhil, M.D., Abass, K.H., Habubi, N.F., Chiad, S.S (2020). "Enhancement of Urbach Energy and Dispersion Parameters of Polyvinyl alcohol with Kaolin Additive" NeuroQuantology 3 66-73.

[39] Abass K. H. and Anas H. H. (2020), "Reduction of Energy Gap in ZrO_2 Nanoparticles on Structural and Optical Properties of Casted PVA–PAAm Blend", Journal of Green Engineering, 10,7,4166–4176.

[40] Dakhil M. Sakhil, Shaban Z. M., Khansaa S. Sh., Habub N. F., Abass K. H., Chiad S. S., Alkelaby A. S. (2020)," Influence MgO Dopant on Structural and Optical Properties of Nanostructured CuO Thin Films", NeuroQuantology ,1, 5, 56-61.

[41] Jumaah, S.H., Hussein, M.R., Habubi, N.F., Chiad, S.S., Abass, K.H (2022), "Improving the Antibacterial Properties of SnO_2/ Mn_3O_4 Hybrid Thin Film Synthesized by Spray Pyrolysis Method", Nano Biomedicine and Engineering,14(3),280–288.

[42] Hamood, F.J., Mohmed, B.Y., Kadim, A.M, Abass, K.H., Agarwal, M.K., Mohammed, K.A (2023). "Effect of CdS Nanoparticles on Structural, Optical and Dielectric Properties for Gamma-Ray Shielding and Antibacterial E±ciency of PVA/PAAm Polymers Blend", International Journal of Nanoscience.

[43] Gouda O. E., Mahmoud S. F., El-Gendy A. A., and Haiba A. S. (2014), "Improving the Dielectric Properties of High-Density

Polyethylene by Incorporating Clay-Nano Filler," TELKOMNIKA Indones. J. Electr. Eng.12,12,7987–7995.

[44] Abd-Alkareem B. (2016), "Effect of Nano-Copper Oxide on the Electrical and Optical Properties of (PMMA) Polymer." M. Sc. thesis, College of Education for pure sciences, University of Babylon.

[45] Shivashankar H., Mathias K. A., Sondar P. R., hrishailM. H. S, and Kulkarni S. M. (2021), "Study on low-frequency dielectric behavior of the carbon black/polymer nanocomposite," J. Mater. Sci. Mater. Electron. 2,28674–2868.

[46] Abass, K.H., Hataf, A.H., Mubarak, T.H., "Effect of Ag nanoparticles on AC electrical parameters of PVA-PAAm and PVA-PMMA-PAAm blends", AIP Conference Proceedingsthis link is disabled, 2023, 2475, 090036.

[47] Yadav L. S. R. (2016), "Electrochemical sensing, photocatalytic and biological activities of ZnO nanoparticles: synthesis via green chemistry route," Int. J. Nanosci.,15, 04, 1650013.